



ICANS-XV  
15<sup>th</sup> Meeting of the International Collaboration on  
Advanced Neutron Sources  
November 6-9, 2000  
Tsukuba, Japan

**23.6**  
**Analytical Study on Structural Integrity of Target Vessel**

H. Kogawa\*<sup>1</sup>, S. Ishikura<sup>1</sup>, M.Futakawa<sup>1</sup>, K.Kikuchi, M.Kaminaga<sup>1</sup> and R.Hino<sup>1</sup>

<sup>1</sup>Japan Atomic Energy Research Institute, Tokai 319-1195, Japan

\*E-mail : [kogawa@cat.tokai.jaeri.go.jp](mailto:kogawa@cat.tokai.jaeri.go.jp)

**Abstract**

Pressure wave is one of critical issues for structural integrity of the mercury target vessel for a MW-class neutron scattering facility. Impact tests on mercury were carried out under high strain rates to estimate the viscosity of mercury and to verify FEM code. An elastic-solid model without dependency on the strain rate could be used to predict impact behaviors in mercury. And, to estimate structural integrity of the target vessel made of stainless steel (the assumed allowable stress of 370.8 MPa), FEM analyses on the pressure wave were carried out under 1 MW (3 GeV, 25 Hz) proton beam condition. It was found that the maximum mises stress of 220.8 MPa was caused by the pressure wave on the outer surface at the center of the window.

**1. Introduction**

In the Japan Atomic Energy Research Institute (JAERI), the neutron scattering facility connecting with a MW-class high-intensity pulse proton beam accelerator is being developed cooperating with the High Energy Accelerator Research Organization (KEK) [1]. The mercury target will be used for this facility from the viewpoint of a good neutron yield and a heat-removable advantage compared to a solid target-water cooling system.

However, mercury has large thermal expansion coefficient and low specific heat, hence, a pressure wave will be induced in mercury by rapid energy depositions due to the pulse proton beam whose pulse duration is 1  $\mu$ s. And it is critical issue for structural integrity of the target vessel because the induced pressure wave is large and is loaded repeatedly, more

than  $10^6$  times, to the target vessel in its lifetime.

The ASTE (the AGS Spallation Target Experiment) collaboration has been carried out to examine the pressure wave generated in the mercury target and the response of the target vessel due to the pressure wave as well as verify analytical codes used for a mercury target design. In this experiment, displacement velocity on the target vessel was measured by a laser-Doppler-vibrometer. The experimental results agreed well with the analytical results by using the Finite Element Method (FEM) analysis until 100  $\mu$ s after the proton beam injection [2]. After 100  $\mu$ s, the response on the displacement velocity of the target vessel became slower in the experimental result than the analytical result. It was considered that the viscosity of the mercury caused this phenomenon.

Impact tests on mercury were carried out to estimate the viscosity of mercury under high strain rate and to verify the FEM code. And then, structural strength of the target vessel was analyzed under 1 MW (3 GeV, 25 Hz) proton beam condition by using the explicit FEM code, LS-DYNA [3]. This paper introduces the mercury impact test results and structural analytical results of the mercury target.

## **2. Liquid mercury behavior and verification of mercury model**

### **2.1 Experiment apparatus and analytical model**

In order to examine the dynamic behavior of the mercury under high pressures and high volume strain rates, impact tests on the liquid mercury were carried out by using a split Hopkinson pressure bar (SHPB) apparatus, as shown in Fig.1. A vessel for mercury was set between the input and output bars. Mercury was carefully poured into the vessel without any air bubbles. The diameter and length of the bars are 10 mm and 1500 mm, respectively. The vessel had enough stiffness to ignore the deformation due to the pressure, and rubber o-rings were installed into between the vessel and the bars; the clearance between outer diameter of the bars and inner diameter of the vessel is about 0.1 mm, to prevent a leakage of the mercury followed by bars moving. Such a stiff vessel may realize a constraint condition as a uniaxial strain condition in the mercury. An impact bar shot by an air gun collides with the input bar to generate the stress wave. The stress wave propagates in the input bar and transmits to the output bar through mercury, loading the pressure wave with high strain rate. Measurements on the stress waves propagating through the bars were taken at the axial centers of each bar by strain gauges. The stress propagation on each bar and liquid mercury were analyzed by using the explicit FEM-code, LS-DYNA, which is used for the design of the target vessel on the pressure wave. Figure 2 shows the three-dimensional FEM model. The mercury was modeled as elastic-solid, where Young's modulus is 6.651 MPa and Poisson's ratio 0.49995 (nearly 0.5), so that the bulk modulus becomes 22.2 GPa.

### **2.2 Results**

Figure 3 (a) and (b) show the strain wave histories of the input and output bars. As seen in these figures, the analytical results agree well with the experimental result. The average axial pressure  $P$  and volumetric strain  $\Delta V/V$  histories in mercury were obtained by using following Kolsky formulas [4] under the uniaxial strain condition;

$$\Delta V/V = \frac{c_0}{l_s} \int_0^t (\varepsilon_i - \varepsilon_t - \varepsilon_r) dt \quad (1)$$

$$P = \frac{AE}{2A_s} (\varepsilon_i + \varepsilon_r + \varepsilon_t) \quad (2)$$

where  $\varepsilon_i$ ,  $\varepsilon_r$  and  $\varepsilon_t$  are stresses propagating through the input and output bars, and  $A$ ,  $E$  and  $c_0$  are sectional area, density and sound speed of the bars, and  $A_s$  and  $l_s$  are sectional area and length of the specimen. Figure 4 shows the relationships between the pressure  $P$  and the volume strain  $\Delta V/V$  in the various impact velocities.  $P$  increased almost linearly with  $\Delta V/V$  in the early stage in any cases. These gradients are independent on the impact velocity and agree with the bulk modulus of mercury, 22.2 GPa.

### 3. Design analyses for mercury target vessel

#### 3.1 Analytical model

Figure 5 shows a three-dimensional FEM model of JAERI/KEK mercury target used for FEM analysis. In Fig.5, the target width, height and length direction are made to be x, y, z-axis, respectively. The target vessel is 800 mm in length, 350 mm in width and 85 mm in height. The shape of window has the curvature in x-direction, whose radius is 800 mm to reduce thermal stress. The vessel was divided into 10,000 shell elements whose thickness is 2.5 mm at window, 5 mm at front wall, and 10 mm at side and top walls except area facing to moderators, whose thickness is 7.5 mm. Inside of the target vessel, 10 mm thick baffle plates were installed as model of distributors for cross flow [1]. Inside of the target vessel was filled with liquid mercury divided into 132,000 solid elements. From the experimental results mentioned above, liquid mercury is modeled as elastic solid without the dependency on the strain rate whose Young's modulus is 6.651 MPa and Poisson's ratio 0.49995 (nearly 0.5) to be bulk modulus is 22.2 GPa, thermal expansion coefficient  $61 \times 10^{-6}$  /K and density 13285 kg/m<sup>3</sup>. The target vessel will be made of austenitic stainless steel, such as type 316L (SS316L) or type 316LN (SS316LN), which Young's modulus is 188 GPa, Poisson's ratio is 0.3, thermal expansion coefficient  $15.3 \times 10^{-6}$  /K and density 7890 kg/m<sup>3</sup>. Temperature dependency and load rate effects for the properties of these materials are not considered in this analysis.

Figure 6 shows energy deposition distribution in the mercury obtained by the Monte Carlo code, NMTC/JAERI under a 3 GeV proton beam (1MW) condition: the proton beam size is 130 x 50 mm and an energy profile is rectangular. Since this energy deposition shows a

time-averaged value, the pulse beam intensity was estimated on the basis of above energy deposition under 25 Hz and 1  $\mu$ s pulse duration. Then, we added the 30% margin to the pulse beam intensity. Temperature rise distribution,  $T(x,y,z)$ , due to the proton beam pulse is estimated by following equations by using the energy deposition distribution expressed by a function,  $f(x, y, z)$ .

$$T(x,y,z) = \frac{f(x,y,z) \times \tau}{c_p \times \rho} \quad \tau \leq 1\mu s$$

$$T(x,y,z) = \frac{f(x,y,z) \times 1 \times 10^{-6}}{c_p \times \rho} \quad \tau > 1\mu s$$

where,  $\tau$  is a pulse duration,  $c_p$  specific heat of mercury (137 J/kg·K) or stainless steel (511 J/kg·K) and  $\rho$  density of mercury or stainless steel. The maximum temperature rise is only 7.6°C at 30 mm apart from the window on the cross sectional center of the target.

### 3.2 Analytical results

Figure 7 shows time responses of pressure wave at the positions where the maximum temperature rise appeared, A, and where mercury contacts with the window center, B. At the position A, the maximum pressure of 33 MPa appears at 1  $\mu$ s after proton injection, which continues while 20  $\mu$ s. Pressure at position B decreases immediately after proton beam injection stops at 1  $\mu$ s. This is because the constraint for the mercury becomes so weak as to make the mercury pressure negative, which would allow free deformation of mercury due to an expansion of the vessel due to pressure wave. These phenomena might induce cavitation on and close to the vessel, which would cause cavitation erosion on the vessel surface.

On the other hand, the vessel is loaded by pressure wave and a stress wave due to the thermal expansion of the vessel itself. Figure 8 shows the stress responses at the center of the window. In this figure, the stresses on the inner surface, the midpoint and the outer surface are shown on x, and y -components. Every stress components show compression of 15 MPa due to the temperature rise in the vessel, and reverses to tensile after the pressure wave propagates to the window so as to expand it. The maximum y-direction tensile stress at the midpoint is 70 MPa at 37  $\mu$ s after the proton beam was injected into the target. The stresses on the outer and inner surface of the window become 150 MPa and -35 MPa (compression) at that time, respectively, due to bending stress. At 160  $\mu$ s after the proton beam injection, the maximum stress of 254 MPa appears on the outer surface, the maximum compression stress of 250 MPa appears on the inner surface.

### 3.3 Structural integrity

The stress on the target vessel due to the pressure wave is assumed as the secondary stress because the pressure wave is generated by the thermal expansion of mercury, that is, the

stress on the target vessel results from the deformation of mercury. Assuming 3 Sm as the allowable stress of the target vessel concerned with the secondary stress, the allowable stress is 345 MPa for SS316L and 414 MPa for SS316LN.

Figure 9 shows the mises stress contour of the vessel on the outer surface at 160  $\mu$ s after the proton beam injection. The maximum mises stress of 220.8 MPa appears at the center of the window.

Other loads including this category are thermal stress induced by a steady thermal load and the stress due to the inner static pressure. The thermal stress generated on the target vessel was estimated by using the ABAQUS/Standard [5] with the same model of the target vessel as shown in Fig.5. The temperature distribution was analyzed using the following parameters;  $\alpha=10000$  w/m<sup>2</sup> of the heat transfer rate from the vessel to mercury, 50 °C of the inlet mercury temperature and  $\lambda = 16.0$  W/m·K of the thermal conductivity of the stainless steel. From the stress analysis carried out by using the temperature distribution data, the maximum mises stress adding the thermal stress to the stress due to the pressure wave was found to be 371.8 MPa at the center of the window.

#### 4. Summary

The impact tests on the mercury using the SHPB apparatus and the design analyses were carried out. From the analytical results with the elastic-solid mercury model, the maximum pressure wave of 33 MPa generated at 30 mm apart from the window on the cross sectional center of the target. And the maximum mises stress of 220.8 MPa was caused by the pressure wave. The maximum mises stress of 371.8 MPa appeared by adding the thermal stress to the stress due to the pressure wave. This value is little over the assumed allowable stress of SS316L, 345 MPa, and below the allowable stress of SS316LN, 414 MPa. Although the maximum mises stress due to the pressure wave is below the assumed allowable stress of SS316L, it has the possibility that the maximum mises stress would be suppressed below the allowable stress of SS316L by decreasing the thermal stress by means of the heat transfer enhancement etc.

As the next step, we will examine the fatigue characteristics of SS316L and SS316LN under loading pressure waves.

#### Reference

- [1] R.Hino, et al. "Spallation Target Development at JAERI - R&Ds on thermo-mechanical design -" ICANS-XIV (1998) pp.252-268.
- [2] M.Futakawa, et al. "Measurement of Pressure Wave in Mercury Target", ICANS-XIV (1998) pp.244-251.
- [3] J.O.Hallquist, "LS-DYNA3D THEORETICAL MANUAL", Japan Research Institute (1994).

[4] K.T.Ramesh, "The Short-Time Compressibility of Elastohydrodynamic Lubricants", J. of Tribology (1991), pp.361-370.

[5] "ABAQUS/Standard ver.5.8", Hibbit, Karlsson & Sorenson, Inc.

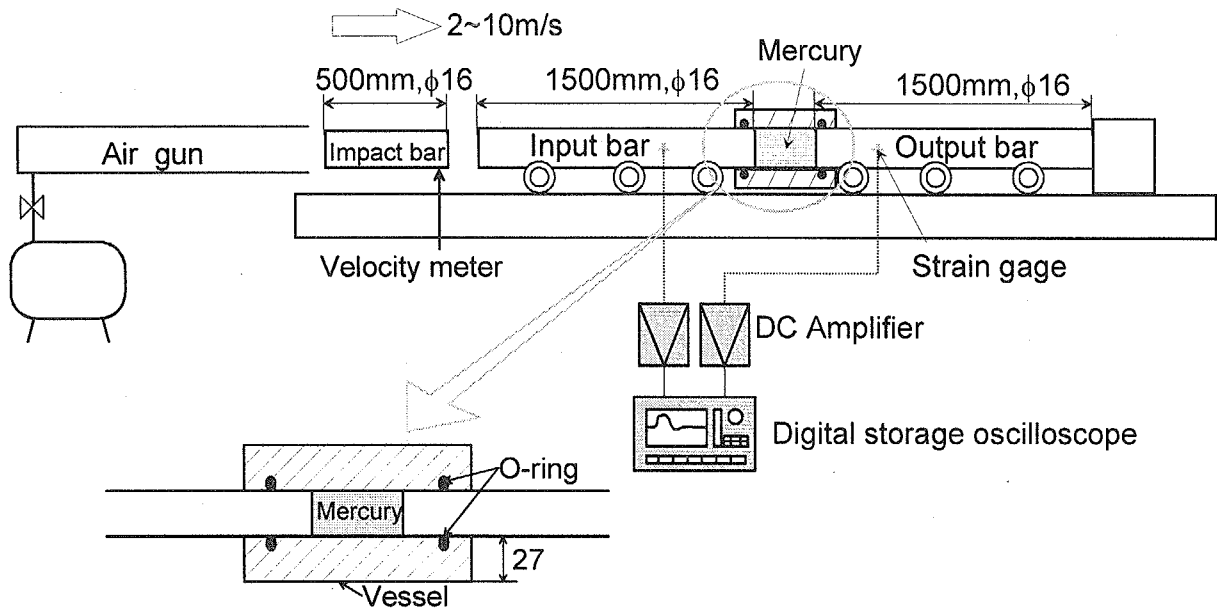


Fig.1 Impact test apparatus

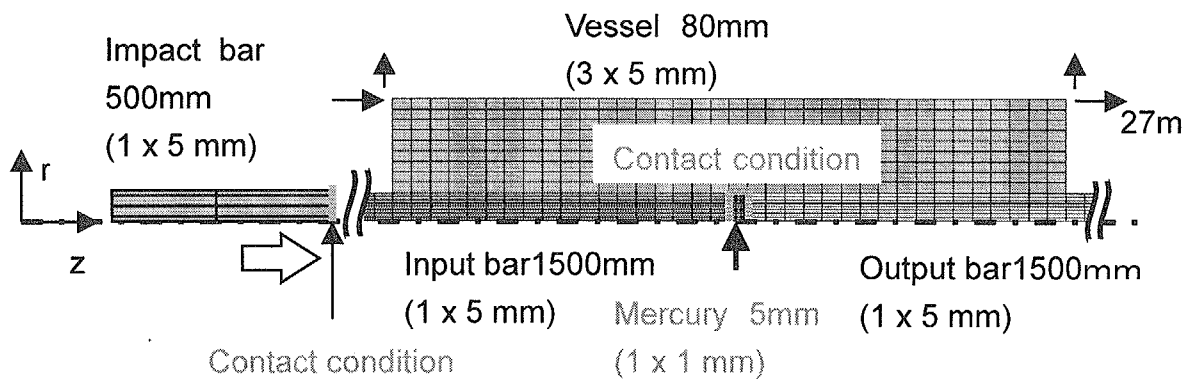
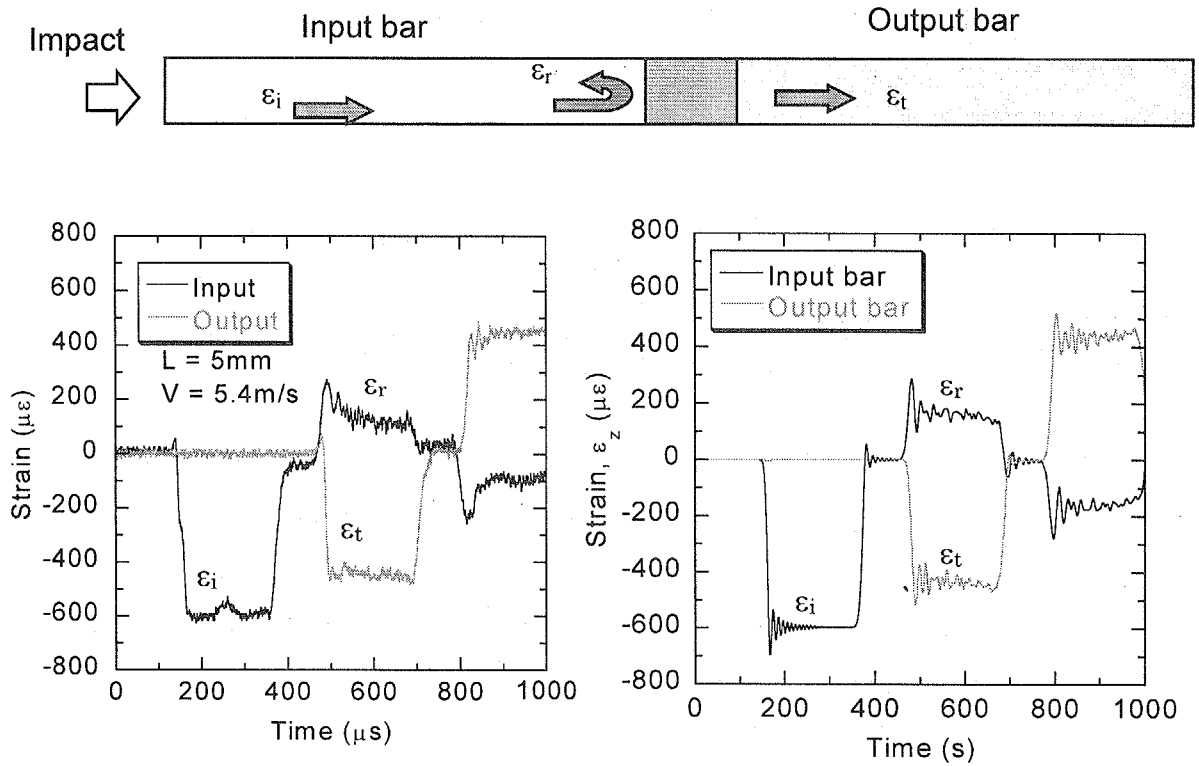


Fig.2 Three-dimensional FEM model for impact test



(a) Experimental results

(b) FEM results

Fig.3 Strain wave in input and output bars on impact test

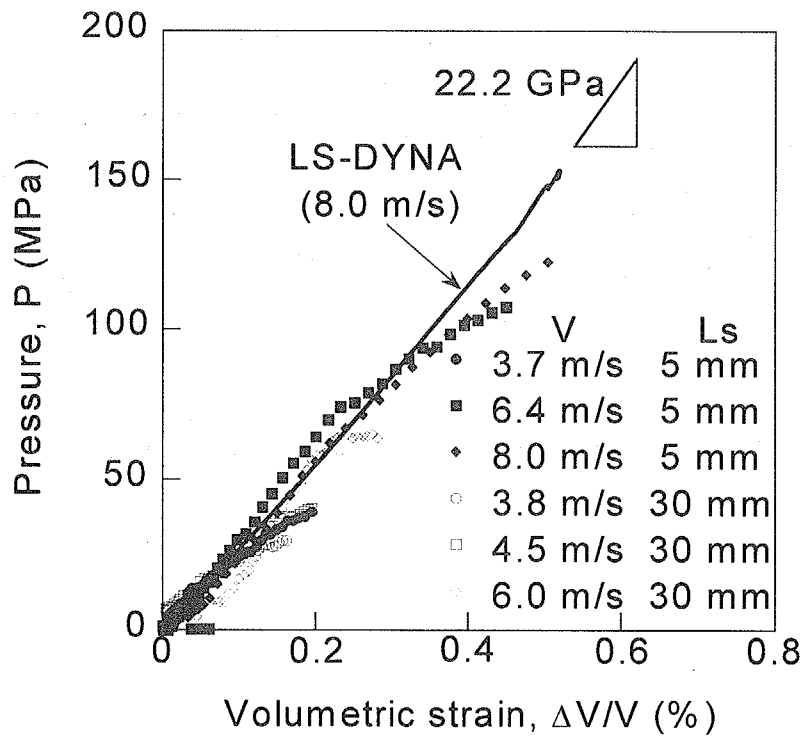


Fig.4 Relationship between pressure and volumetric strain of mercury

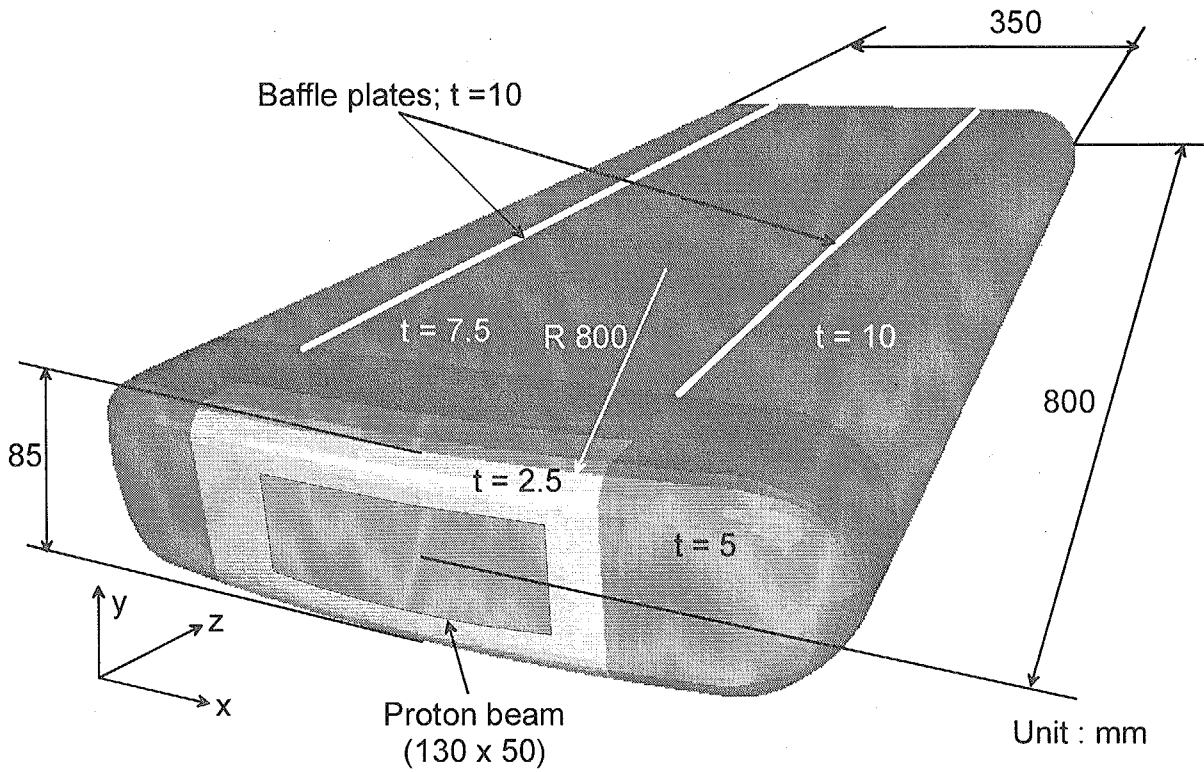


Fig.5 Three-dimensional FEM model of JAERI/KEK mercury target

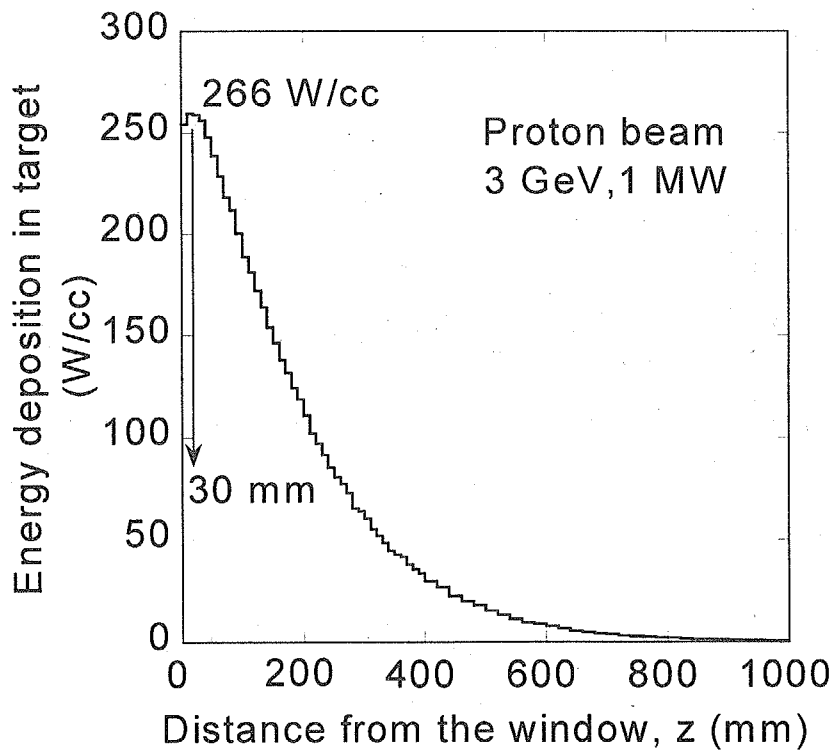


Fig.6 Energy deposition distribution in mercury target



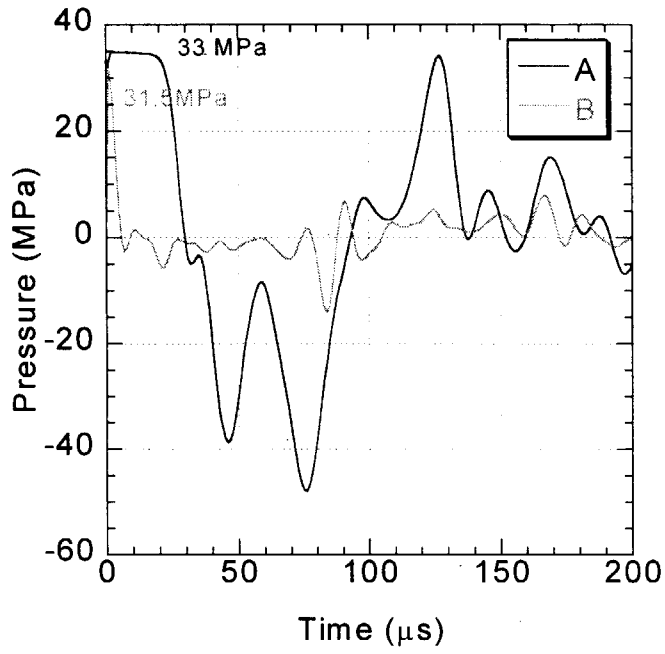


Fig.7 Time response of pressure wave in mercury

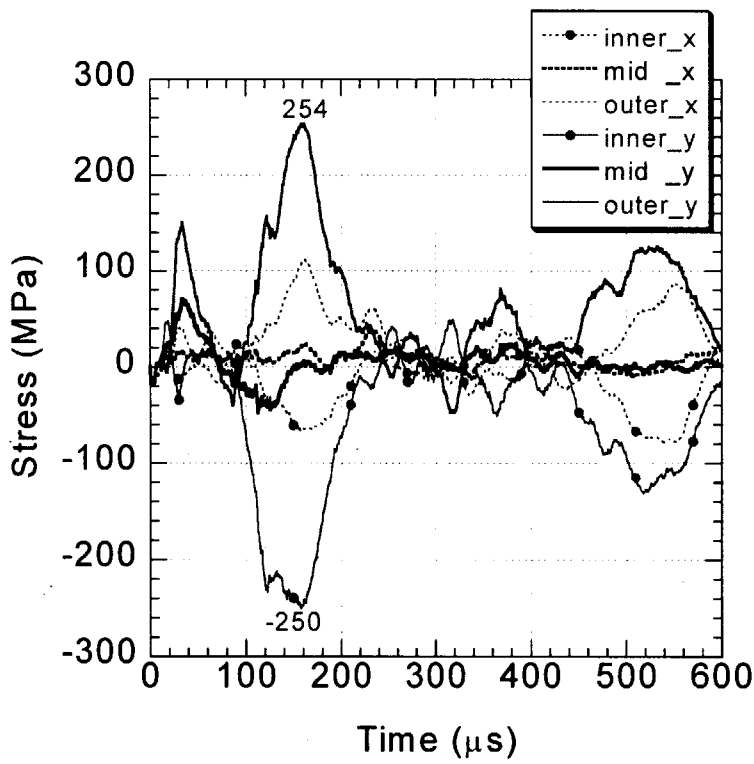


Fig.8 Stress responses at center of window

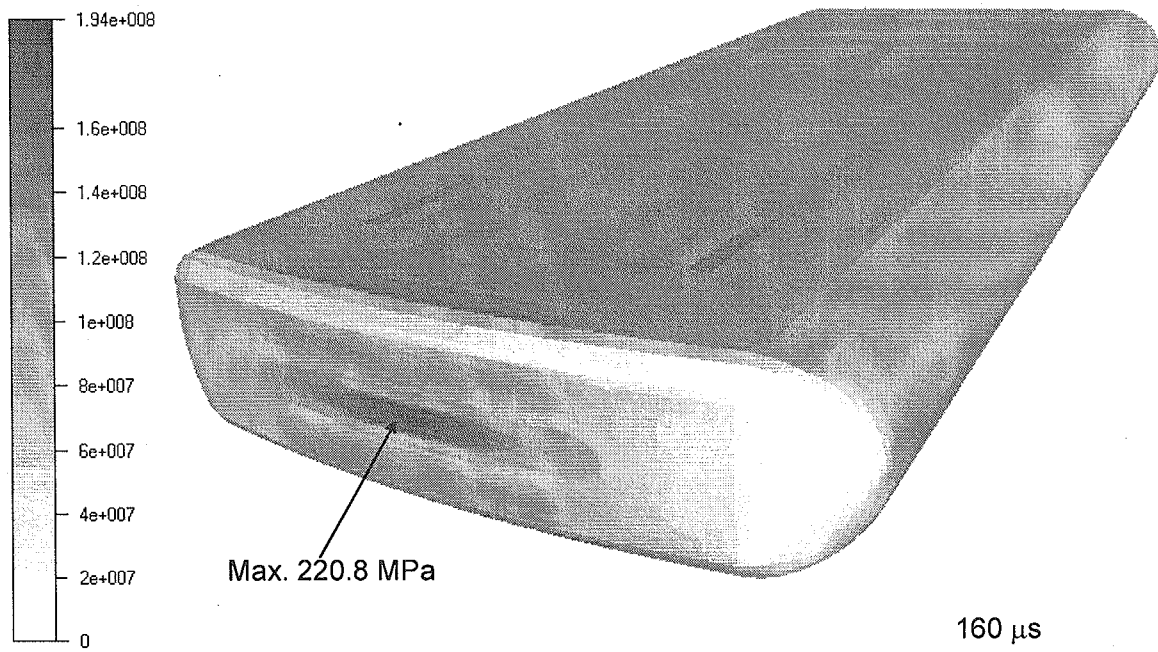


Fig.9 Mises stress contour of the vessel on outer surface at 160 μs after proton beam injection